Title:	**Stack Effect in High-Rise Buildings: A Review**
Authors:	Stefano Cammelli, BMT Fluid Mechanics Ltd. Sergey Mijorski, SoftSim Consult Ltd.
Subject:	Sustainability/Green/Energy
Keywords:	Natural Ventilation Passive Design Stack Effect
Publication Date:	2016
Original Publication:	International Journal of High-Rise Buildings Volume 5 Number 4
Paper Type:	1. Book chapter/Part chapter 2. **Journal paper** 3. Conference proceeding 4. Unpublished conference paper 5. Magazine article 6. Unpublished

International Journal of High-Rise Buildings
December 2016, Vol 5, No 4, 327-338
http://dx.doi.org/10.21022/IJHRB.2016.5.4.327

International Journal of
High-Rise Buildings
www.ctbuh-korea.org/ijhrb/index.php

Stack Effect in High-Rise Buildings: A Review

Sergey Mijorski[1] and Stefano Cammelli[2,†]

[1]*SoftSim Consult Ltd., Mladost-4, bl.438, ap.14, Sofia, 1715, Bulgaria*
[2]*BMT Fluid Mechanics Ltd., 67 Stanton Avenue, Teddington, TW11 0JY, United Kingdom*

Abstract

This technical paper presents a detailed review of the stack effect phenomenon and of the associated implications pertaining to the design and construction of high-rise buildings in regions of extreme climatic conditions. The present review is focused on both the classical 'chimney' effect as well as on the reverse stack effect, which are respectively related to cold and hot climates. For the purposed of the work here presented, the ASHRAE (2013) design conditions of Astana (Kazakhstan) and Riyadh (Kingdom of Saudi Arabia) were selected. A 230 m tall residential building of rectangular floor plan was numerically modelled in the context of the climatic conditions of the two abovementioned cities and a number of sensitivity analyses were performed, covering parametric changes of: temperature, façade air tightness, site wind speeds and wind directions.

Keywords: Stack effect, Buoyancy, High-rise building, Multi-zone air flow modelling, Façade air tightness, Flow rate

1. Introduction

The stack effect is a buoyancy-driven phenomenon that commonly occurs in high-rise buildings. This physical phenomenon typically arises in regions experiencing extreme climatic conditions. The main driver behind the stack effect phenomenon is the temperature difference between the interior of the building and the external environment. Also, the impact of wind pressure acting on the external envelope of the building should not be ignored as it can be a significant contributor to the overall building performance.

1.1. Buoyancy-driven Processes

In cold regions, the relatively warmer indoor air of a tall building rises due to buoyancy forces, creating a pressure difference that tries to draw air in at the bottom of the building and pushes air out at the top levels. The cold air that has been drawn in is then heated up by the building services, closing the cycle of the classical stack effect process (see illustrative diagram in Fig. 1(a)).

On the other hand, in hot climates, a reverse process can be observed: in this case the relatively cooler indoor air of a high-rise building precipitates, creating a pressure build-up around the lower portion of the building that pushes the air out and draws the air in at the upper levels. Again, the warm air that has been drawn in is then cooled down by the building services, closing the cycle of the 'reverse' stack effect process (see illustrative diagram in Fig. 1(b)).

It should be noted that in both types of stack effect processes there is usually a change in sign (direction) of the pressure gradient at the building envelope: this indicates that, at some point along the height of the building, there is a zone of neutral pressure where the internal and external pressures are perfectly equalized.

1.2. Wind-driven Processes

Additionally to the buoyancy force, it is also important to take into account the impact of the wind pressure acting on the envelope of the building. It is well known that, due to the shape of the atmospheric boundary layer, the lower and upper levels of tall buildings are subjected to rather different wind speeds (wind pressures). This can have a non-negligible impact on infiltration and exfiltration through the skin of the building; in particular, positive external wind pressures have the ability of enhancing infiltration and counteracting exfiltration whilst negative external wind pressures have the ability of enhancing exfiltration and counteracting infiltration (see Fig. 2).

1.3. Design Challenges

The main design challenges associated with the stack effect phenomenon in tall buildings are:

- Elevator doors operation: elevator doors, due to excessive pressure difference across them, could malfunction and not operate correctly within their guide rails;
- Swing doors operation: users, due to the excessive pressure difference across swing doors, could experience difficulties in opening / closing them;
- Uncomfortable and / or excessive air flow movement: this has the potential to occur within key occupied

†Corresponding author: Stefano Cammelli
Tel: +44-20-8614-4400; Fax: +44-20-8943-3224
E-mail: scammelli@bmtfm.com

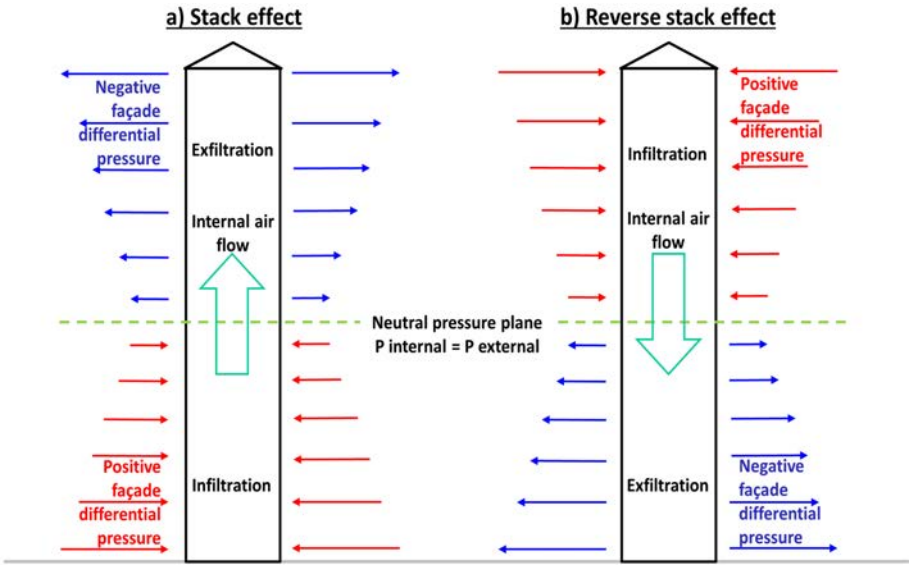

Figure 1. Principle stack effect diagrams.

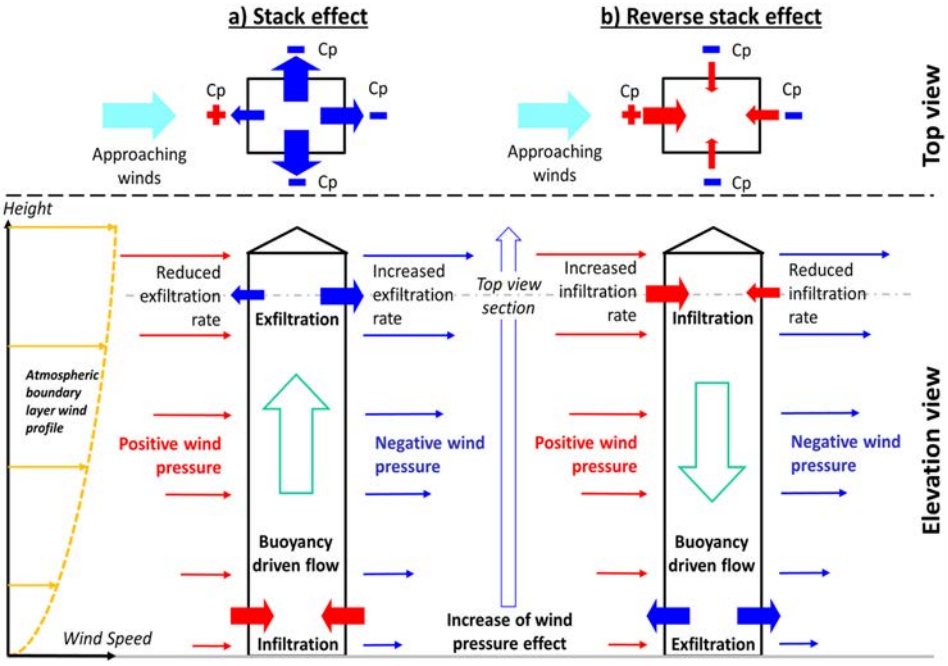

Figure 2. Wind pressure impact over building stack effect.

spaces such as lobbies, corridors, atria, etc.;

- Propagation / spreading of smoke, odors and other unwanted contaminants throughout the building;
- Inefficient heating / cooling strategy: because of the excessive infiltration of cold (hot) ambient air into the lower (upper) levels of the tall buildings, extra energy supply is likely to be required to heat up (cool down) such spaces;
- Flow-borne noise: high speed air flow through narrow gaps (e.g., door gaps, louvers of the shafts or natural ventilation openings) could be the cause of narrow-band high pitch whistling which in turn can create discomfort to the occupants of the tall building;
- Fire strategy: an excessive air flow movement within the tall building could increase the propagation rate of smoke and fire. Also, excessive deviation from prescribed pressurization levels along the main evacuation paths (e.g., stairwells and corridors) due to stack

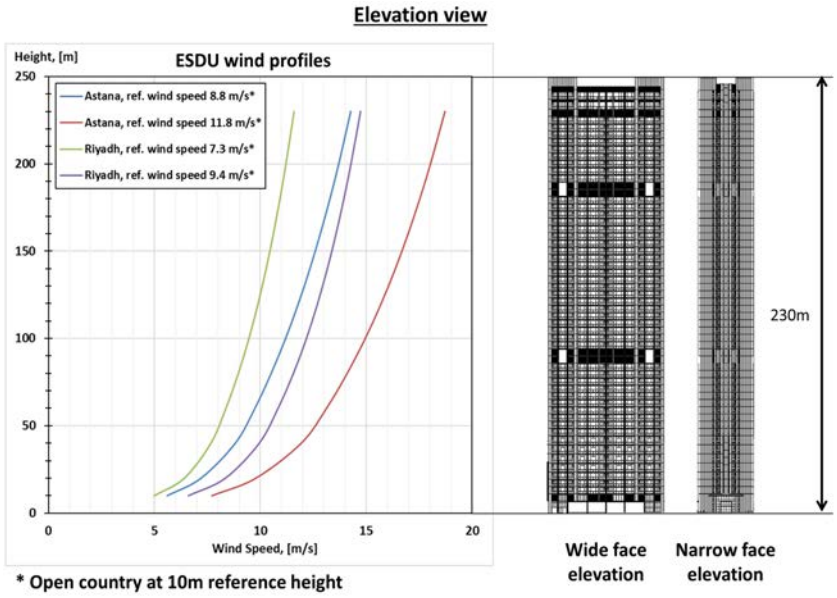

Figure 3. Building elevation and wind profiles.

effect, could impede smooth occupants' evacuation procedures to take place.

1.4. Preventive Measures

In order to prevent some of the issues listed above, the following measures should be considered / implemented (Jo et al. 2007):

- Improvement of the quality and air tightness of the building envelope (from design to on-site QA/QC through detailed technical specification);
- Installation of revolving doors at key access points to the building;
- Implementation of vestibules between building entrances and elevator banks;
- Introduction of vertical separations within elevators and stairwell shafts;
- Introduction of horizontal separations (e.g., additional internal partitioning);
- Improvement of the air tightness of the elevator machine room;
- Implementation of mild pressurization within elevators and stairwell shafts;

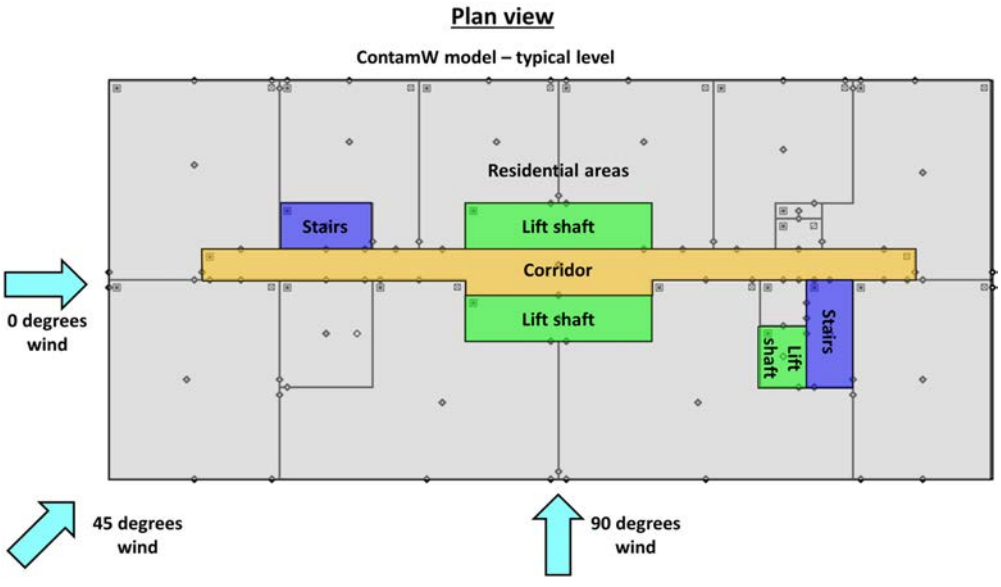

Figure 4. Building plan and approaching winds.

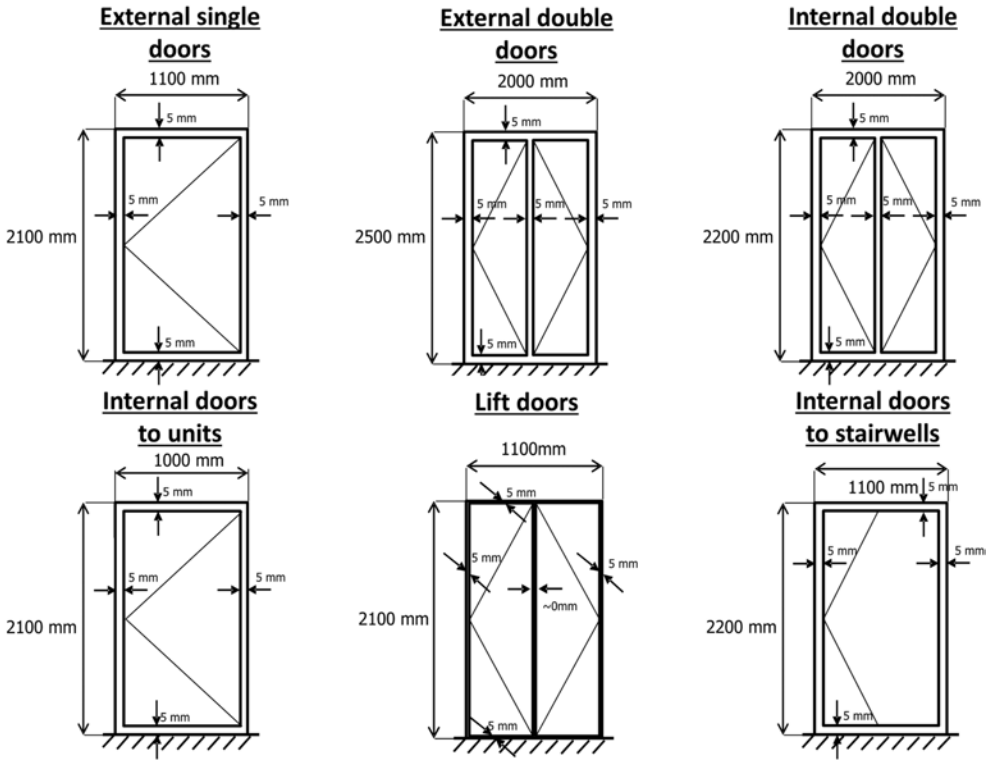

Figure 5. Door specifications.

- Modification and control of the design temperature within elevators and stairwell shafts.

2. A Case Study

2.1. General Information

For the purposes of this technical paper, a 63-storey / 230 m tall residential building of rectangular floor plan was selected. The elevation of the building, together with a graphical representation of the approaching wind profiles, are illustrated in Fig. 3.

Two cities of extreme climatic conditions were considered:

- Astana (Kazakhstan): extreme winter conditions (stack effect);
- Riyadh (Kingdom of Saudi Arabia): extreme summer conditions (reverse stack effect).

Within this technical paper only three wind directions were considered, namely 0, 45 and 90 degrees, as illustrated in Fig. 4. Also shown in the Fig. 4 are the main internal zones of a typical residential level of the building.

2.2. Wind Pressures

The aerodynamic roughness lengths assumed for the city center of Astana and Riyadh were respectively 0.7 m and 0.5 m. The site-specific mean wind speed profiles have been determined using ESDU (2001), whilst the magnitude and the distribution of the external mean wind pressures over the building envelope were calculated following Eurocode (2005).

2.3. Building Elements and Construction Specifications

The doors considered in this study were specified with a uniform door-to-frame gap size of 0.005 m and thickness of 0.05 m (see Fig. 5), whilst all internal walls and floor areas (shaft and partitioning) were classified, as either low, medium or high air flow resistant elements (see Table 1 for the actual porosity levels), following the specification of ASHRAE (2013).

Regarding the façade specifications, the following international standards were considered:

- American Society for Testing and Materials (ASTM 2012);
- Russian code (СНиП 2011);
- Eurocode (EN 2012);
- Chinese code (GB/T 2007).

Table 1. Porosity levels of the internal walls and partitioning (ASHRAE 2013, Chapter 16, Ventilation and Infiltration, Table 10)

Walls	Porosity - Total opening area per square meter
High air flow resistant walls	0.14×10^{-4} m/m
Medium air flow resistant walls	0.11×10^{-3} m/m
High air flow resistant walls	0.35×10^{-3} m/m
Floor/ceilings	0.52×10^{-4} m/m

Table 2. Façade properties

Façade Specification	Façade Leakage
American code: ASTM E283	0.948 m/m·h at 300 Pa
Russian code: СНиП 23-02-2003 Code	0.5 kg/m^2·h at 121.3 Pa
Eurocode: EN 12152:2002 Code	Class A4: 1.5 m^3/m^2·h at 600 Pa
Chinese code: GB/T 21086-2007	Grade 4: 0.5 m^3/m^2·h at 10 Pa

Further details of the air leakage properties are given in Table 2.

2.4. Hvac Systems

Heating, ventilation and air conditioning (HVAC) systems were considered in operation at all building's levels for all simulated cases. For a typical level of the tall building, an air supply / extraction of 0.9 m^3/s and 0.8 m^3/s were respectively chosen. For the entire building, the total supply of air was approximately 50 m^3/s, whilst the air extracted approximately 42 m^3/s. Also, the interior design air temperature was set to 21°C for the winter scenarios and 23°C for the summer cases.

3. Multi-zone Air Flow Numerical Model

For the purposes of the present technical paper, the computer program CONTAMW 3.2 – a multi-zone airflow and contaminant transport analysis software developed by the National Institute of Standards and Technology (NIST) – was utilized. A detailed review of the validation of CONTAMW can be found in Emmerich (2001), whilst information related to the CONTAMW multi-zone modelling can be found in Dols and Polidoro (2015).

A detailed CONTAMW network flow model of the proposed building was constructed and configured with all the required flow paths and boundary conditions. The model included all lift shafts, stairwells and occupied spaces and incorporated a detailed representations of the airtightness of the building envelope, internal / external doors and internal partitioning.

3.1. Flow Paths Modelling

Flow paths (façade, walls, doors, slabs, shafts, etc.) can be numerically modelled through the assignment of specific leakage rates, wall porosity and flow resistance or through the specification of an appropriate door-to-frame/ window-to-frame gap size. In the analysis work presented within this technical paper, power law and quadratic model were utilized to describe the performance of such flow paths with regard to leakage at different levels of pressure differential. Details of the mathematical models pertaining to different types of flow paths can be found in Dols and Polidoro (2015).

In the multi-zone air flow numerical model described within this technical paper, the different flow paths were modelled as follows:

- Façade: modelled through a power law based on a single test data point with a reference differential pressure of 300 Pa and a flow exponential of 0.65;
- Walls and internal partitions: modelled through a power law based on a given leakage area at a differential pressure of 75 Pa, a flow exponential of 0.65 and a discharge coefficient of 0.6;
- Doors: modelled through a quadratic model in the form of $DP = a \cdot Q + b \cdot Q^2$, where Q is the volume flow rate as per Baker et al. (1987). This model takes into account the total length of the door crack, the gap size (in this case 0.005 m) and the thickness of the door (in this case 0.05 m);
- Stairwells: modeled through a power law based on flow resistance fitted to experimental data as per Achakji and Tamura (1988);
- Lift shafts: modelled through a power law based on a flow resistance calculation performed according to a friction model that uses the Darcy-Weisbach relationship and the equation of Colebrook for friction factors as documented in "Chapter 21 - Duct Design" of ASHRAE (2013);

3.2. Scenarios Matrix

The steady state winter and summer conditions, respectively for Astana and Riyadh, were based on ASHRAE (2013) and are summarized in Tables 3(a) to 3(c). Three types of sensitivity analyses were performed: one focused on varying the outdoor ambient temperature (see Table 3(a)); one focused on varying the strength and directionality of the wind speed (see Table 3(b)); and one focused on varying the air tightness of the façade system (see Table 3(c)).

4. Numerical Results And Discussion

The discussion of the numerical results presented within this technical paper are subdivided in the following sections:

- Baseline models;
- Sensitivity to ambient temperature;
- Sensitivity to wind speed and wind direction;
- Sensitivity to façade airtightness.

The graphical results are presented in Fig. 6 through to Fig. 13; these include the floor-by-floor total net air infiltration / exfiltration as well as the maximum pressure difference across the different levels of the building, which is defined as the largest difference between the maximum and minimum pressure differential experienced across any particular floor.

4.1. Baseline Models

The baseline conditions selected for the two sites were

Table 3. Scenario matrix

(a) Impact of ambient temperatures

Case	Season	Site Location	DB [°C]	Wind speed [m/s]	Wind direction [°]	Façade Specification
Astana, 5-yr return period temperature	Winter (baseline)	ASTANA, Kazakhstan	-37	8.8	0°	ASTM code
Astana, 50-yr return period temperature	Winter	ASTANA, Kazakhstan	-42.9	8.8	0°	ASTM code
Riyadh, 5-yr return period temperature	Summer (baseline)	RIYADH, Saudi Arabia	46.7	7.3	0°	ASTM code
Riyadh, 50-yr return period temperature	Summer	RIYADH, Saudi Arabia	48.2	7.3	0°	ASTM code

(b) Impact of approaching winds

Case	Season	Site Location	DB [°C]	Wind speed [m/s]	Wind direction [°]	Façade Specification
Astana, 5% exceedance wind speed, 0°	Winter (baseline)	ASTANA, Kazakhstan	-37	8.8	0°	ASTM code
Riyadh, 5% exceedance wind speed, 0°	Summer (baseline)	RIYADH, Saudi Arabia	46.7	7.3	0°	ASTM code
Astana, 1% exceedance wind speed, 0°	Winter	ASTANA, Kazakhstan	-37	11.8	0°	ASTM code
Riyadh, 1% exceedance wind speed, 0°	Summer	RIYADH, Saudi Arabia	46.7	9.4	0°	ASTM code
Astana, 5% exceedance wind speed, 90°	Winter	ASTANA, Kazakhstan	-37	8.8	90°	ASTM code
Riyadh, 5% exceedance wind speed, 90°	Summer	RIYADH, Saudi Arabia	46.7	7.3	90°	ASTM code
Astana, 5% exceedance wind speed, 45°	Winter	ASTANA, Kazakhstan	-37	8.8	45°	ASTM code
Riyadh, 5% exceedance wind speed, 45°	Summer	RIYADH, Saudi Arabia	46.7	7.3	45°	ASTM code

(c) Impact of façade specification

Case	Season	Site Location	DB [°C]	Wind speed [m/s]	Wind direction [°]	Façade Specification
ASTM code façade	Winter (baseline)	ASTANA, Kazakhstan	-37	8.8	0°	ASTM code
Russian code façade	Winter	ASTANA, Kazakhstan	-37	8.8	0°	СНиП code
EN code façade	Winter	ASTANA, Kazakhstan	-37	8.8	0°	EN code, class A4
Chinese code façade	Winter	ASTANA, Kazakhstan	-37	8.8	0°	Chinese code, grade 4

as follows: 5-yr return period Dry Bulb Temperature (DBT), 5% exceedance wind speed, 0 degrees wind direction and façade specification based on the ASTM code (see Table 3(a)).

Fig. 6 presents the floor-by-floor net air infiltration/exfiltration thought the building envelope, whilst Fig. 7 shows the floor-by-floor minimum (associated with the leeward and side faces of the building) and maximum (associated with the windward face of the building) differential pressure across the different façade elements of the building taking into account both the external wind pressures and the pressures driven by the stack effect phenomenon.

Fig. 6 shows a relatively high level of mass flow rate at the upper and lower levels of the building, where direct sizeable connections between the internal spaces of the building and the atmosphere are located. More specifically, in Astana baseline case, the air infiltrates at the bottom of the building and it is withdrawn at the top, with a neutral pressure plane of the building located between 'Level 7' and 'Level 9'. On the other hand, in Riyadh baseline case, the air is withdrawn at almost all building's levels (with the exception of 'Level 60'): this is because the buoyancy forces in this specific case are 'only' driven by a temperature difference of approximately 23°C (as opposed to 58°C in Astana), making the contribution of the negative external wind pressures acting on the envelope of the building and the effect of the HVAC system positively pressurizing its interior spaces far more dominant. This also explains the absence of an actual neutral pressure plane.

The graph pertaining to Astana in Fig. 7 shows predominately negative differential pressures acting across the building envelope: these are primarily the result of negative external wind pressures acting in sync with the buoyancy-driven forces. Not only: there is also a large difference between the minimum and the maximum differential pressures experienced across any given floor (approxi-

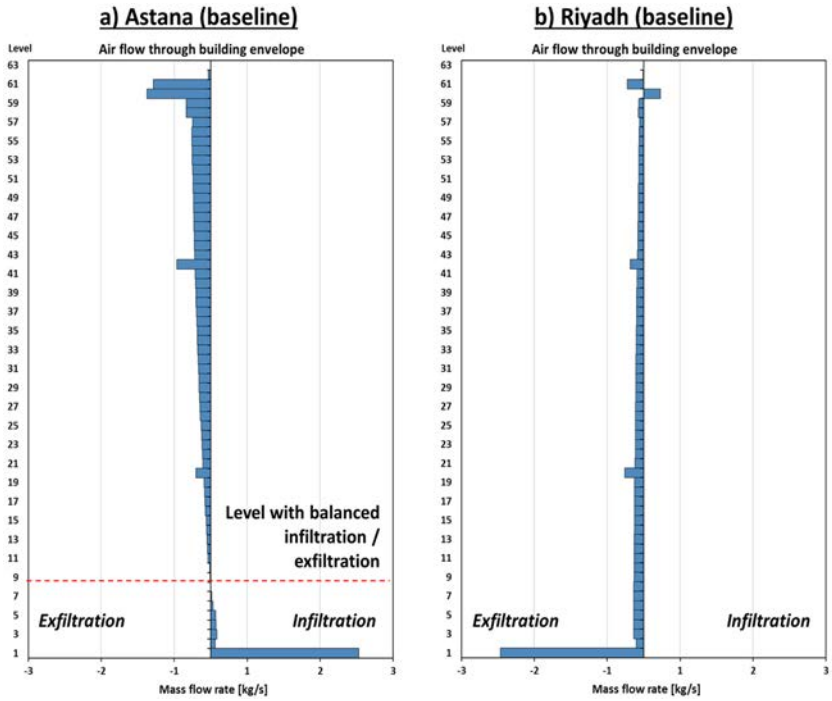

Figure 6. Baseline models - Net air infiltration / exfiltration through the building envelope; (a) Astana, (b) Riyadh.

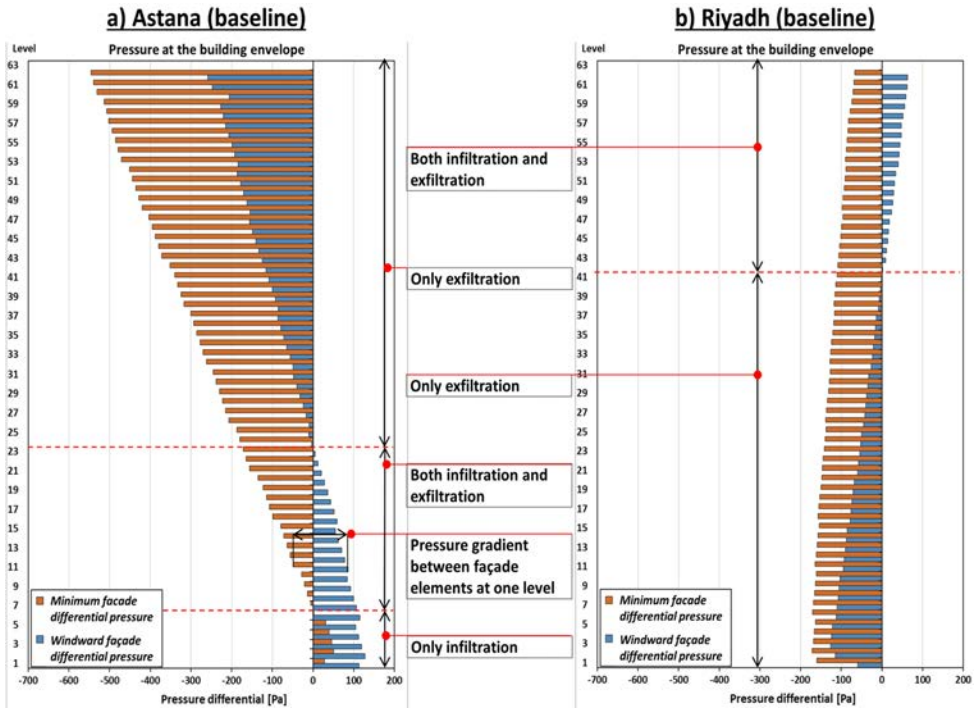

Figure 7. Baseline models - Minimum and maximum pressure differential across the building envelope; (a) Astana, (b) Riyadh.

mately up to 300 Pa), especially towards the top of the building. On the other hand, in Riyadh, the buoyancy forces do tend to act against the negative external wind pressures acting on the skin of the building, improving the

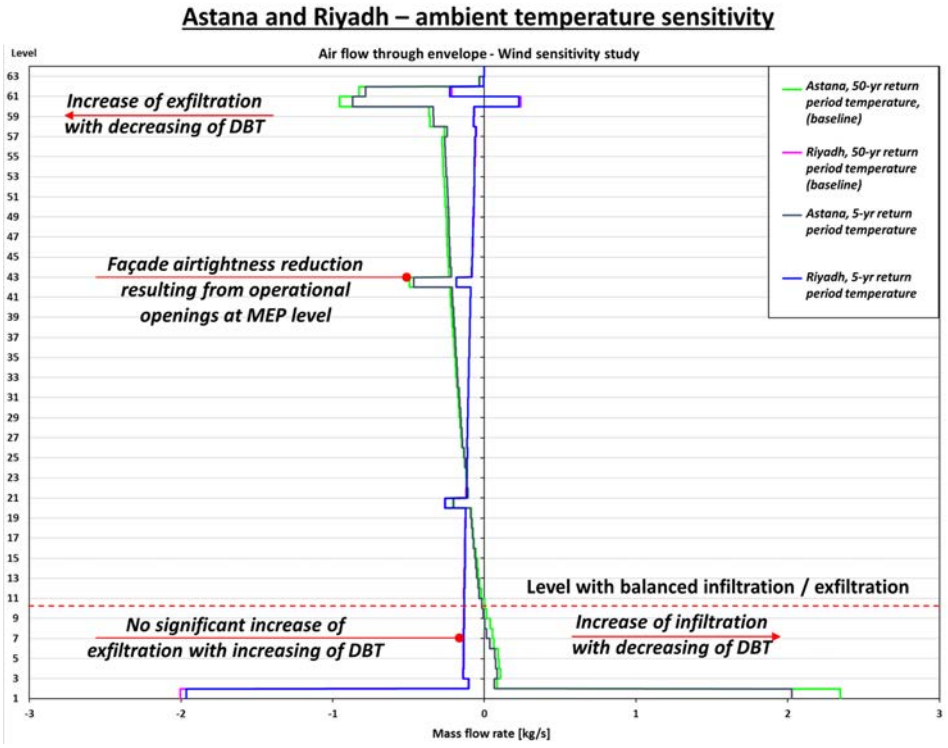

Figure 8. Astana and Riyadh (sensitivity to ambient temperature) - Net air infiltration / exfiltration through the building envelope.

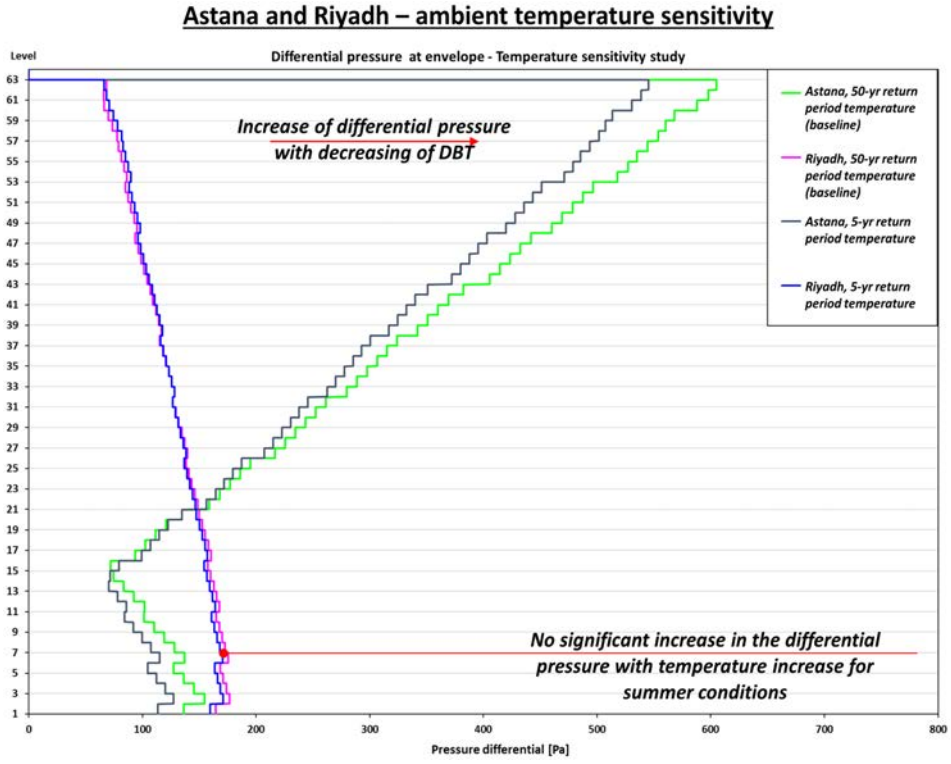

Figure 9. Astana and Riyadh (sensitivity to ambient temperature) - Maximum pressure difference across the entire levels of the building.

overall building performance.

4.2. Sensitivity to Ambient Temperature

The impact of changes to the ambient temperature was assessed by comparing, at both sites, two different design conditions, namely the 5-yr and the 50-yr return period DBT.

In Astana, the change of DBT from -37ºC to -42.9ºC increased the infiltration at 'Ground Level' and the exfiltration at 'Level 60', as shown in Fig. 8. However, for all other levels the changes were relative minor. At the same time, as shown in Fig. 9, this change in DBT has led to an increase of the maximum pressure difference across the different floors of the building: however, due to the good airtightness specification of the building façade, this increase didn't cause significant contribution to the net infiltration and exfiltration with except of the two localized levels mentioned above.

In Riyadh, the overall impact of temperature change was assessed to be small, both from a net infiltration and exfiltration rates point of view (see Fig. 8) and from a maximum pressure difference perspective (see Fig. 9).

4.3. Sensitivity to Wind Speed and Wind Direction

The impact of the different wind conditions on the stack effect phenomenon was assessed by comparing, at both sites, two different design conditions – 5% and 1% exceedance wind speeds, and three different wind directions – 0, 45 and 90 degrees. The results, which are graphically presented in Figs. 10 and 11, show a remarkable increase of the maximum pressure difference – especially across the upper levels of the building – as a direct consequence of the increase in wind speed/external wind suction. More specifically, in Astana, the increased level of maximum pressure difference also translated into an increase of the level of net exfiltration over the top portion of the building.

Contrary, in Riyadh, there was no significant increase of maximum pressure difference at most levels.

4.4. Sensitivity to Façade Airtightness

This sensitivity analysis – which compared four different façade type specifications (ASTM, Eurocode, Russians and Chinese specifications) – was only performed for the winter conditions of Astana (5-yr return period DBT and 5% exceedance wind speed). The results are summarized in Figs. 12 and 13.

Fig. 12 shows that the 'Chinese Grade 4' façade is clearly the most permeable one: this resulted in a significant increase of the net infiltration and exfiltration levels throughout the entire building. All other façade types perform significantly better. Of particular interest is the non-negligible upward shift of the neutral pressure plane exhibited by the 'Chinese Grade 4' façade. Additionally, Fig. 13

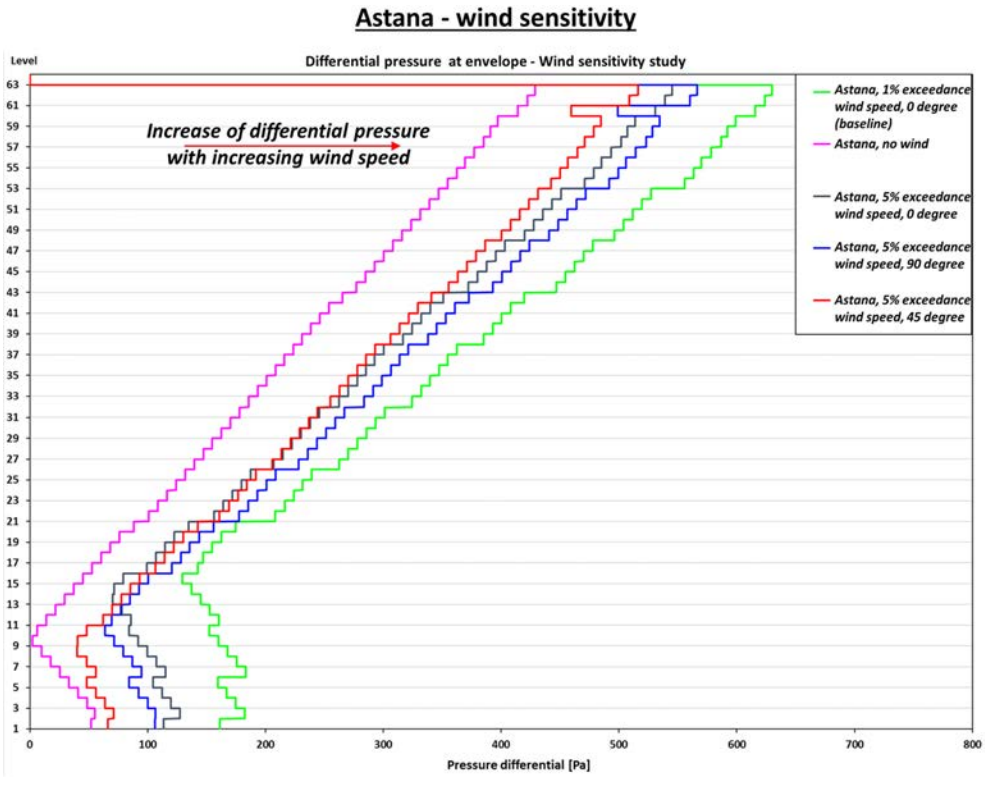

Figure 10. Astana (sensitivity to wind speed and wind direction) - Maximum pressure difference across the entire levels of the building.

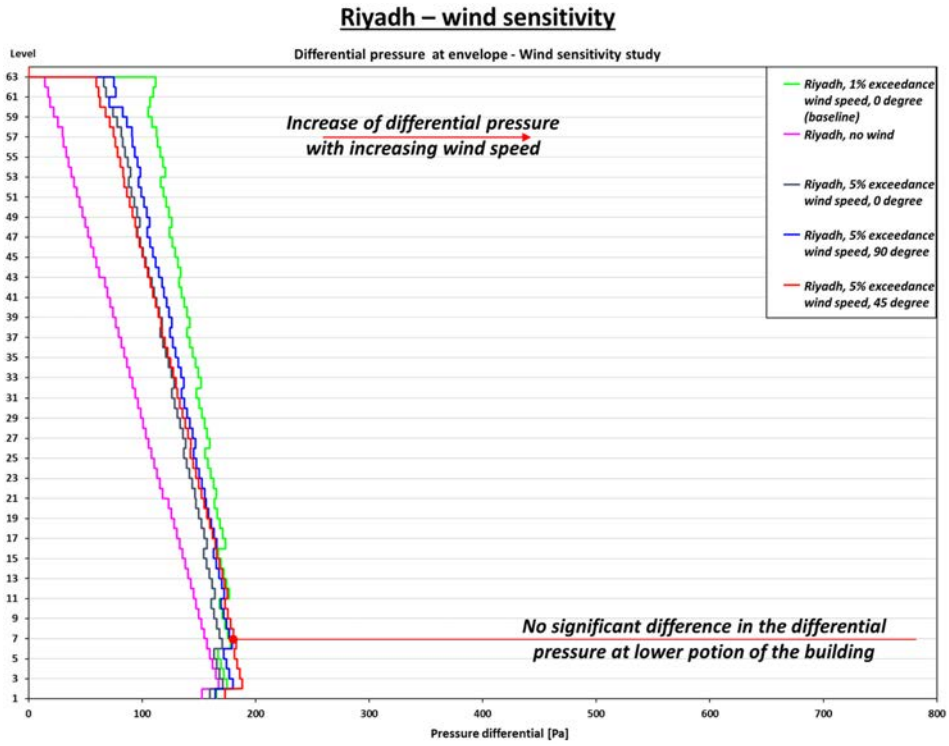

Figure 11. Riyadh (sensitivity to wind speed and wind direction) - Maximum pressure difference across the entire levels of the building.

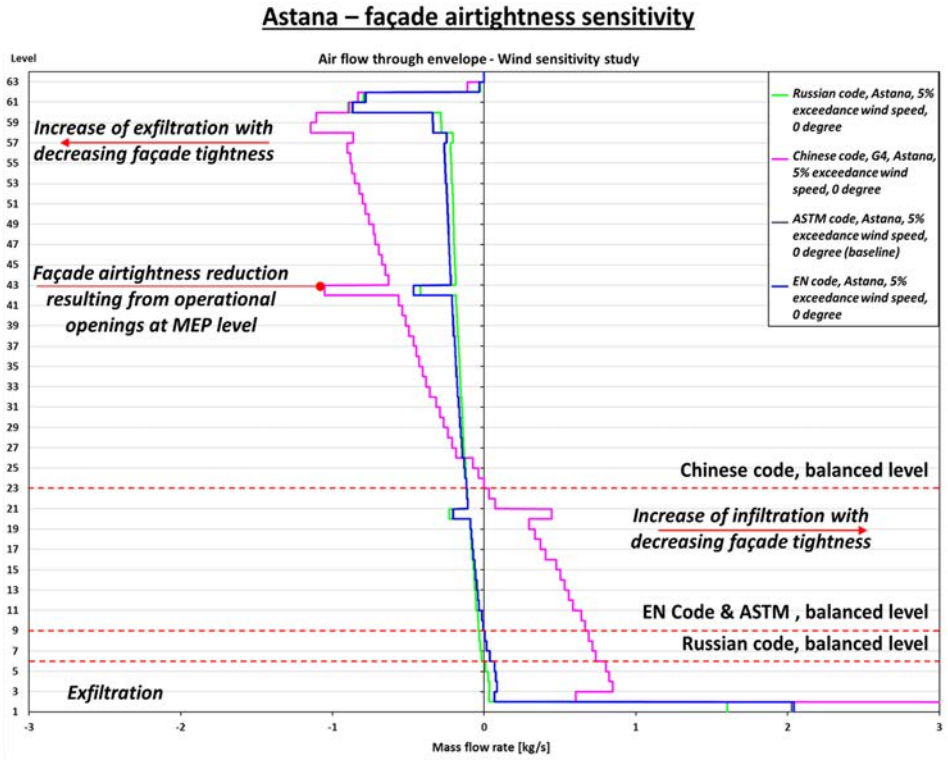

Figure 12. Astana (sensitivity to façade airtightness) - Net air infiltration / exfiltration through the building envelope.

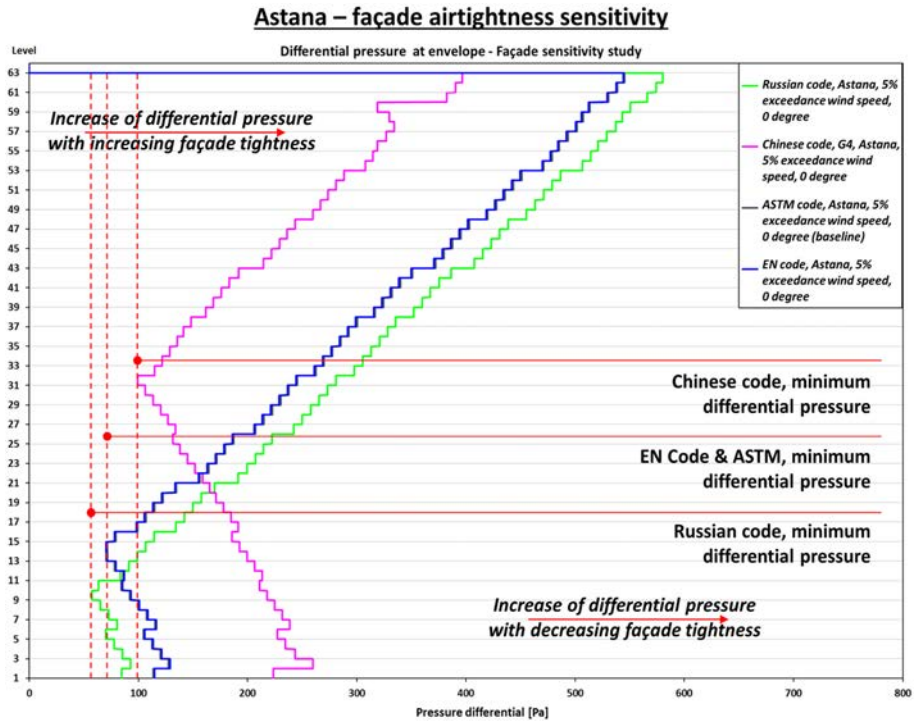

Figure 13. Astana (sensitivity to façade airtightness) - Maximum pressure difference across the entire levels of the building.

shows how the best performing façade types have the ability of holding the highest pressure differentials, especially over the upper levels of the building.

5. Conclusions

The stack effect is a buoyancy phenomenon driven by high temperature differences between the internal spaces of a building and the external environment and as such, harsh winter conditions have the potential to lead to the most challenging operational conditions. However, summer conditions should not be ignored. In this technical paper it was observed that the wind pressures can also play a significant role in the overall buildings' performance.

For relatively simple prismatic buildings, in the case of classical stack effect, wind pressures would typically contribute to enhancing the exfiltration rates across the upper levels of the building. On the other hand, in the case of reverse stack effect, it was observed that wind pressures do tend to counteract the effect of the buoyancy forces.

Another important factor – if not the most important one – that can control the overall performance of a building in relation to stack effect, is the airtightness specification of the façade system. Poor performing façades can only provide low air flow resistance and this, in turn, can lead to: higher infiltration and exfiltration rates through the building envelope; excessive air movement across internal flow paths; low occupant comfort levels; excessive pressure differentials across internal swing / lift doors which could as well lead to operational difficulties; inefficient and uneconomical use of the HVAC system; poor performing smoke propagation control strategy; and sub-optimal performance of the emergency ventilation which could as well lead to an ineffective fire safety strategy for the building.

References

Achakji, G.Y. and Tamura, G.T. (1988). *Pressure Drop Characteristics of Typical Stairshafts in High Rise Buildings*. ASHRAE Transactions, 94(1): 1223-1236.

ASHRAE (2013). *ASHRAE Handbook - Fundamentals 2013*.

ASTM (2012). *ASTM E283: Standard Test Method for Determining Rate of Air Leakage Through Exterior Windows, Curtain Walls, and Doors Under Specified Pressure Differences Across the Specimen*.

Baker, P.H., Sharples, S., and Ward, I.C. (1987). *Air Flow through Cracks*, Building and Environment, Pergamon, 22(4): 293-304.

Dols, S.W. and Polidoro, B.J. (2015). *CONTAM User Guide and Program Documentation*. NIST Technical Note 1887, Version 3.2n.

Emmerich, S.J. (2001). *Validation of Multizone IAQ Modeling of Residential-Scale Buildings: A Review*, National Institute of Standards and Technology, Gaithersburg, MD. ASHRAE Transactions 2001, V. 107, Pt. 2. CI-01-8-1.

EN (2005). *EN 1991-1-4: Eurocode 1: Action on structures - Part 1-4: General actions wind actions.*

EN (2012). *EN 12152: Curtain walling - Air permeability - Performance requirements and Classification.*

ESDU (2001). *Computer program for wind speeds and turbulence properties: flat or hilly sites in terrain with roughness changes - Data Item 01008.* Engineering Science Data Unit, Item 01008.

GB/T (2007). *GB/T 21086-2007: Curtain wall for Building.*

Jo, J.-H., Yeo, M.-S., and Kim, K.-W. (2007). *Effect of Building Design on Pressure-related Problems in High-rise Residential Buildings*. ARCC Spring Research Conference, Eugene, Oregon.

СНиП (2011). *СНиП 23-02-2003: Тепловая защита зданий,* Актуализированная редакция. Министерство регионального развития, Российской Федерации.